

# We are IntechOpen, the world's leading publisher of Open Access books Built by scientists, for scientists

4,800

Open access books available

122,000

International authors and editors

135M

Downloads

Our authors are among the

154

Countries delivered to

TOP 1%

most cited scientists

12.2%

Contributors from top 500 universities



WEB OF SCIENCE™

Selection of our books indexed in the Book Citation Index  
in Web of Science™ Core Collection (BKCI)

Interested in publishing with us?  
Contact [book.department@intechopen.com](mailto:book.department@intechopen.com)

Numbers displayed above are based on latest data collected.  
For more information visit [www.intechopen.com](http://www.intechopen.com)



# Modeling of Air Pollution at Airports

*Oleksandr Zaporozhets and Kateryna Synylo*

## Abstract

Although airports provide several benefits for our society, communities in the vicinity of airports are subjected to the deterioration of air quality. Currently, the basic objects of attention are NO<sub>x</sub> and ultrafine PM due to airport-related emissions. Considered environmental problems are intensified in connection with increasing air traffic, rising tensions of airports expansion and growing cities closer and closer each other, and accordingly growing public concern with air quality around the airport. Aircraft are the dominant and special source of emission and air pollution at airports in most cases under consideration. So, to evaluate the aircraft contribution in LAQ assessment of the airports accurately, it is important to take in mind few features of the aircraft during their landing-takeoff cycle (LTO), which define emission and dispersion parameters of the considered source. The complex model PolEmiCa allows the calculation of the inventory and dispersion parameters of the aircraft engine emissions during the LTO cycles of the aircraft in the airport area. But a clear quantification of aircraft emission contribution to total air pollution is the actual task for development of cost-effective strategies to improve local air quality according to the vicinity of the airport, and to meet regulatory requirements.

**Keywords:** aircraft engine emission, exhaust gases jet, airport air pollution, local air quality, modeling of air pollution, emission inventory

## 1. Introduction

Despite significant economic and social benefits the aviation brings, its activities also contribute to local air quality impact and correspondingly affect the health and quality life of people living near the airports. The number of flights has increased by 80% between 1990 and 2014 and is forecasted to grow by a further 45% between 2014 and 2035. Consequently, the future growth in the European aviation sector will be inextricably linked to its environmental sustainability [1].

During the last decade, a lot of studies have also focused on the aircraft emissions impact on local and regional air quality in the vicinity of airport [2–7]. The basic objects of attention are extremely high concentration of toxic compounds (including nitrogen oxides (NO<sub>x</sub>), particle matter (PM with various sizes: PM<sub>10</sub>, PM<sub>2.5</sub>, and ultrafine), unburned hydrocarbons (UHC), and carbon monoxide (CO)) due to airport-related emissions and their significant impact on the environment [2, 8] and health of the people living near the airport [3, 4].

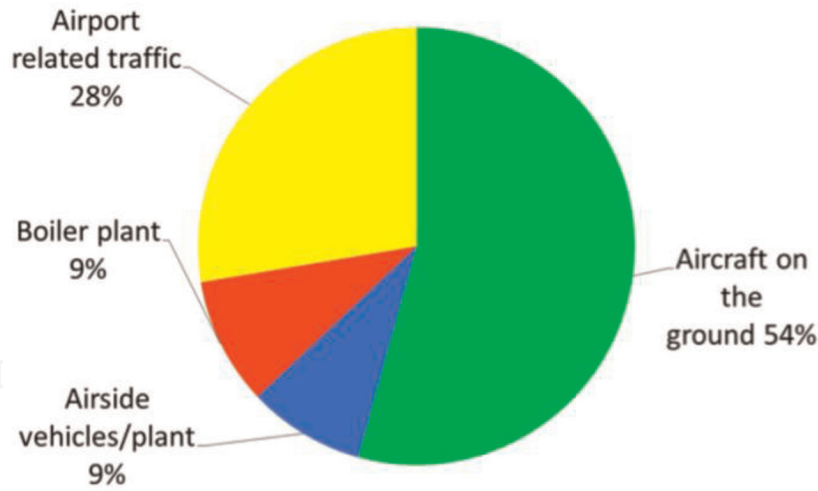
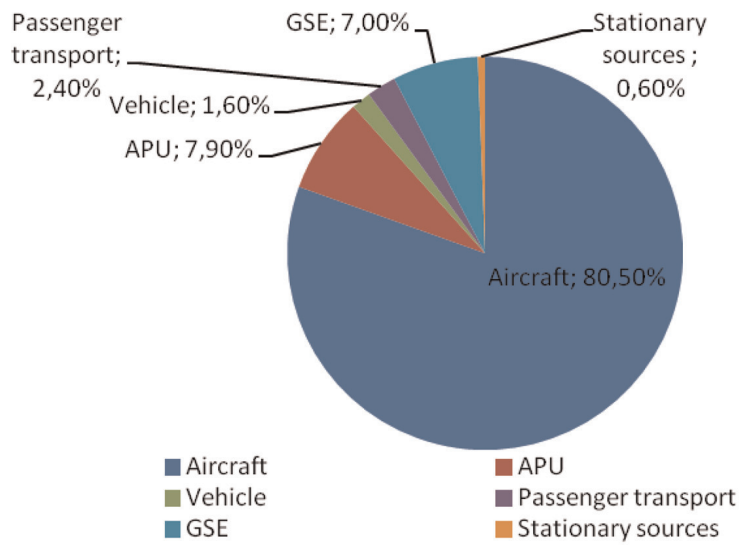
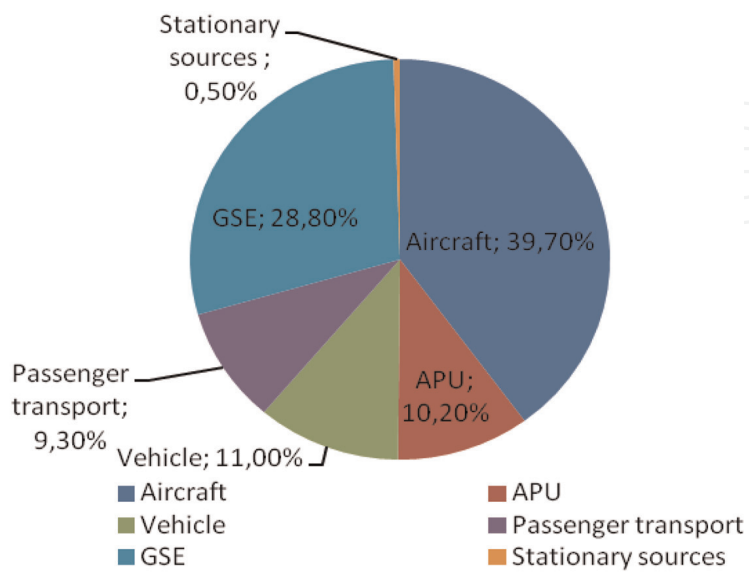


**Figure 1.**  
Estimated ground-level airport-related emissions from Heathrow Airport.



a



b

**Figure 2.**  
The emissions inventory of  $\text{NO}_x$  [(a) annual emissions: 3.284 tons/year] and  $\text{PM}_{10}$  [(b) total emissions: 25 tons/year] within the Frankfurt International Airport for 2005 with an intensity of takeoffs and landings, 1300 per day.

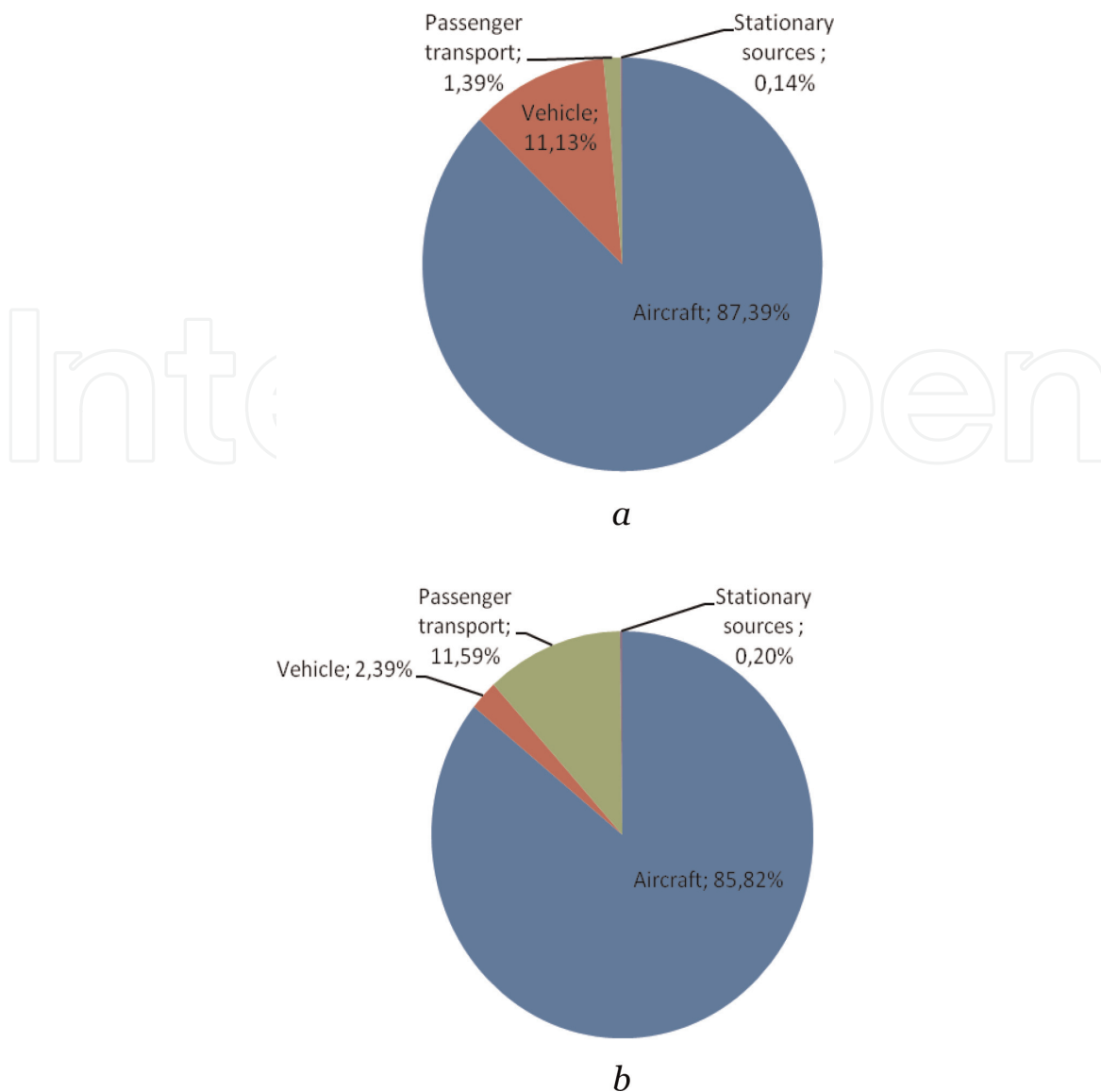


**Figure 3.** The emissions inventory of NO<sub>x</sub> (a) and PM<sub>10</sub> (b) within Boryspil International Airport with an intensity of takeoffs and landings 50,000 per year.

Ground-level emissions associated with the airport have the biggest impact on local air quality, whereas elevated aircraft emissions have less impact because they take place at increasing height. **Figure 1** shows aircraft produce approximately 54% of ground-level emissions, whereas airport-related traffic is estimated to emit a further 28% [5].

Analysis of inventory emission results at major European (Frankfurt am Main, Heathrow, Zurich, etc.) and Ukrainian airports highlighted that aircrafts (during approach, landing, taxi, takeoff and initial climb of the aircraft, engine run-ups, etc.) are the dominant source of air pollution in most cases under consideration [6, 9, 10], **Figures 2** and **3**. More than 50% of total NO<sub>x</sub> emissions inventory inside airport area is released by aircraft engines. As shown in **Figures 2(b)** and **3(b)**, the contribution of aircraft emission to total airport PM emissions is sufficiently high.

Considered problems are intensified in connection with rising tensions of expansion of airports and growing cities closer and closer each other (the most urgent is for Ukrainian airports, such as Zhulyany, Boryspil, Lviv, Odessa, and Zaporizhzhia) and accordingly growing public concern with air quality around the airport.

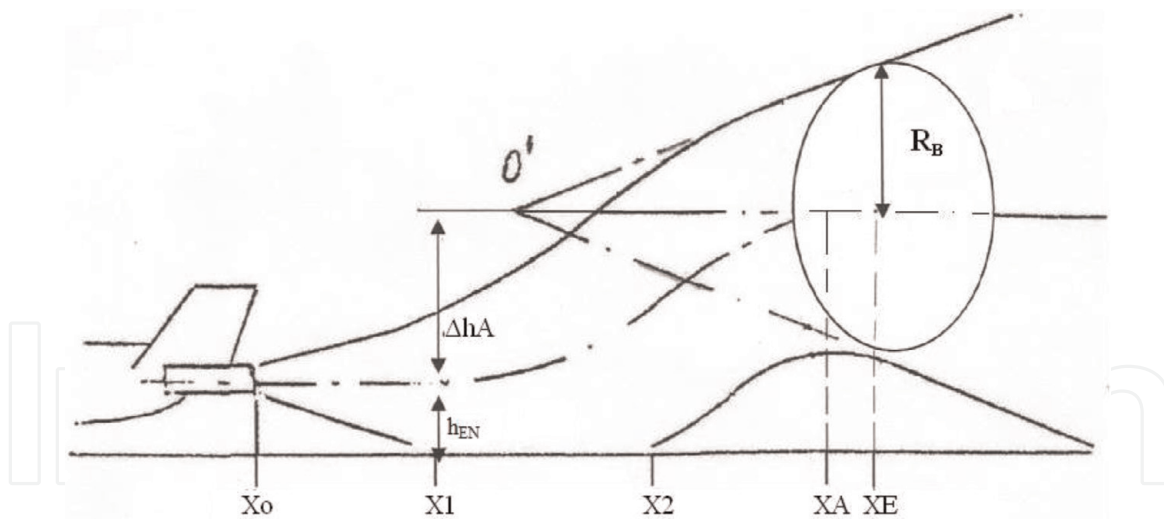


**Figure 4.**

*Jet structure for jet transport model.  $\Delta h_A$ ,  $X_A$  are the height and longitudinal coordinate of jet axis rise due to buoyancy effect, m;  $h_{EN}$  is the height of engine installation, m;  $R_B$  is the radius of jet expansion, m;  $X_1$  is the longitudinal coordinate of first contact point of jet with ground, m; and  $X_2$  is the longitudinal coordinate of a point of jet lift-off from the ground due to buoyancy effect, m.*

Aircrafts are a special source of air pollution due to some features.

**First of all**, aircrafts are a moving (on the ground and in flight) pollution source with varying emission factors during landing and takeoff (LTO) as well as ground operation (engine start after maintenance and run-ups to check the correct operation of the flight system). At the airport, engine operation may change from idle to maximum thrust. Accordingly, temperature, exhaust gas velocity, and emissions of an aircraft engine may change within a wide range [11].

**Second**, the most important feature is the presence of a jet of exhaust gases, which can transport pollutants over rather large distances because of high exhaust velocities and temperatures (**Figure 4**). Such a distance is determined by the engine power setting and installation parameters, mode of airplane movement, and meteorological parameters. The results of jet model calculations show that depending on initial data, the jet plumes from aircraft engines range from 20 to 1000 m and sometimes even more [11].

So, to evaluate the aircraft contribution in Local Air Quality assessment of the airports accurately, it is important to take in mind few features of the aircraft during their landing-takeoff cycle (LTO), which define emission and dispersion parameters of the considered source.

## 2. Modeling of air pollution produced by aircraft engine emissions

Modeling of airport air pollution includes two parts: emission inventory and dispersion calculation.

ICAO Doc 9889 [12] recommends few tools for air quality analysis—to model emission inventory from every character groups of the spatially distributed sources as well as atmospheric concentrations resulting from emission dispersion: EDMS is based on Gaussian plume model (AERMOD) [13], LASPORT is based on Lagrangian particle model (LASAT) [14], and ALAQS-AV provides to use both Gaussian and Lagrangian approaches for dispersion calculations [12].

A complex model Pollution and Emission Calculation (PolEmiCa) for assessment of air pollution and emission inventory analysis, produced within the airport boundaries, has been developed at National Aviation University (Kyiv, Ukraine) [15]. It consists of the following basic components:

1. **engine emission model**—emission assessment for aircraft engines, including influence of operational factors;
2. **jet transport model**—transportation of the contaminants by the jet plume from the engine exhaust nozzle; and
3. **dispersion model**—dispersion of the contaminants in atmosphere due to turbulent diffusion and wind transfer.

## 2.1 Emission model

The emission inventory of aircraft emissions are usually calculated on the basis of certificated emission indexes, which are provided by the engine manufacturers and reported in the database of the International Civil Aviation Organization (ICAO) [16].

The emission indices rely on well-defined measurement procedure and conditions during aircraft engine certification. Under real circumstances, however, these conditions may vary and deviations from the certificated emission indices may occur due to the impact factors such as

- the life expectancy (age) of an aircraft—emission of an aircraft engine might vary significantly over the years (the average period is 30 years); usually aging aircraft/engine provides higher emission indices in comparison with same type but new ones;
- the type of an engine (or its specific modification, for example with different combustion chambers) installed on an aircraft, which can be different from an engine operated in an engine test bed (during certification); and
- meteorological conditions—temperature, humidity, and pressure of ambient air, which can be different for certification conditions.

So, the analysis of several measurement campaigns for idling aircraft at different European airports (London-Heathrow in 1999 and 2000, Frankfurt/Main in 2000, Vienna in 2001, and Zurich in 2003) [7] concludes that the largest difference between emission indices' measurement data and the ICAO data for CO for the RB211-524D4 engine was caused due to quite long life expectancy of B747-236 (aging aircraft and engines) (**Figure 5**). The oldest aircraft with an emission index of 52.9 g/kg was 25 years old; the other two were built in 1987 and 1983. Mean values

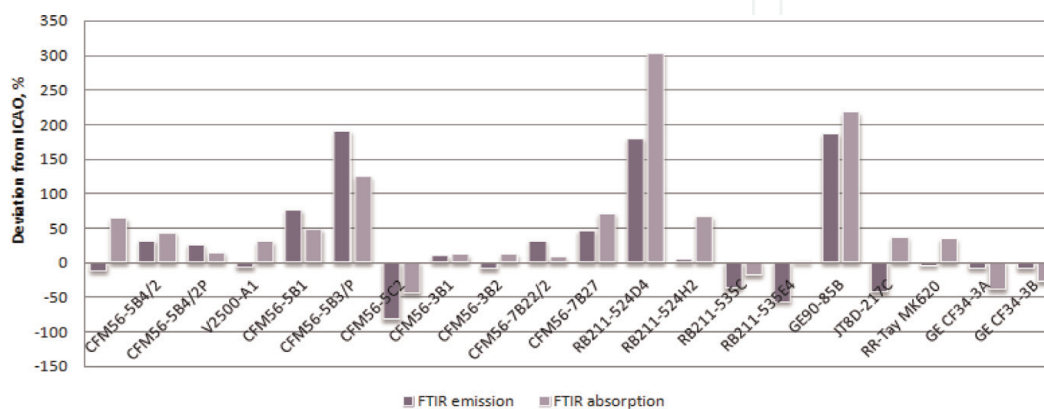


**Figure 5.** Comparison measured  $EI_{CO}$  by FTIR emission and absorption spectrometry during measurement campaign for idling aircraft at the European airports.



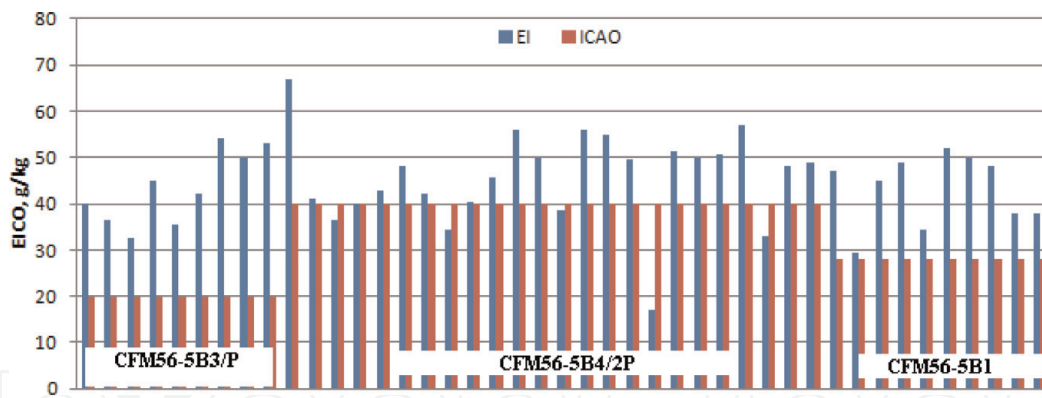


**Figure 6.** Comparison  $EI_{CO}$  determined for CFM-5Bx engines with ICAO values for idling aircraft at European airports.

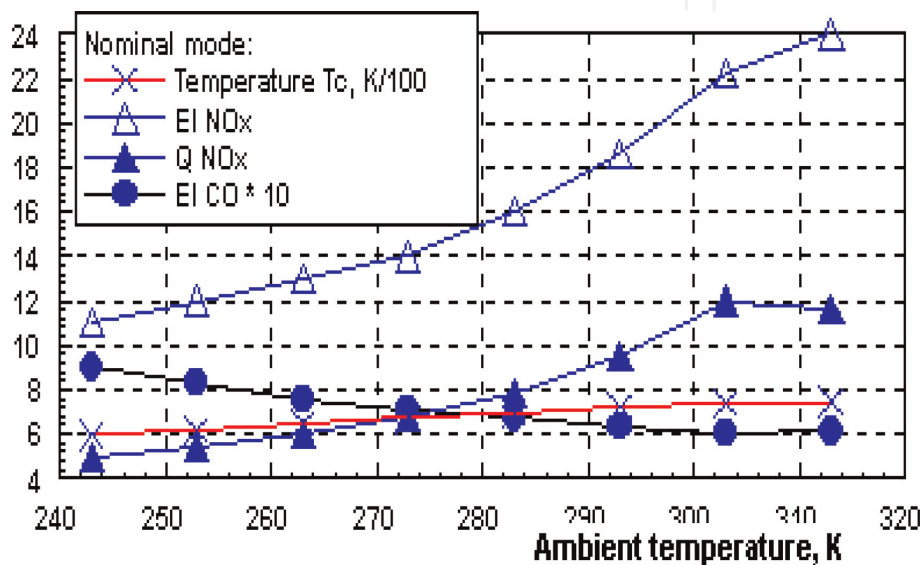


**Figure 7.** Dependences of EE index  $EI$  [ $g_{\text{emission}}/kg_{\text{fuel}}$ ], factor  $Q$  [ $g/s$ ] for  $NO_x$  and temperature behind the compressor  $T_c$  for D-36 engine from ambient temperature.

of the measured emission indices for three engine types (CFM56-5B1, CFM-5B4/2P, and CFM56-5B3/P) are nearly identical although the ICAO data of the CFM56-5B family differ by a factor of 2 (**Figure 6**) [7].

The dependences of engine thermodynamic parameters and EE index for  $NO_x$  (assessed in  $g/kg_{\text{fuel}}$ ) and factor  $Q$  (assessed in  $g/\text{sec}$ ) for the aircraft engine D-36 (installed on Yakovlev-42 and on Antonov-74, -148, and -158 aircrafts) are shown in **Figure 7** as the functions from ambient temperature  $T_A$  (basic engine control law for D-36 provides the constant value of compressor pressure ratio  $\pi_{\Sigma}^*$  in a broad range of ambient temperatures). Values of an emission index  $EI_{NO_x}$  vary up to 50% in relation to value at International standard atmosphere conditions inside the range of ambient temperatures between  $-30$  and  $+30^\circ\text{C}$  [17, 18].

A gradient of change of the factor  $Q_{NO_x}$  at  $T_A < T_{ALIM}$  is also large enough (with  $T_A$  growth, a factor  $Q_{NO_x}$  monotonically increases). In case of change of engine automatic control mode at  $T_A > T_{ALIM}$ , the propellant consumption drops with the growth of temperature; therefore, monotonic character for  $Q_{NO_x}$  dependence disappears and at  $T_A > 30^\circ\text{C}$ , the factor  $Q_{NO_x}$  decreases [17, 18].

So, under operating conditions, engine emission characteristics are subject to changes as a result of influence of the meteorological factors.

Based on the obtained research outcomes of aircraft engine emission derivation, due to meteorological factor influences, the model was developed to recalculate the emission indices for ISA conditions  $EI_{ISA}$  into actual meteorological conditions  $EI_{it}$  [17, 18]:

$$K_{EI} = \frac{EI_{it}}{EI_{iISA}} \quad (1)$$

For emission factor (in g/s or kg/hour), the recalculation into actual meteorological conditions are determined under the formula:

$$K_{Qi} = K_{EI} \cdot \left( \frac{T_t}{T_{ISA}} \right)^{1/2} \quad (2)$$

In **Table 1**, the correction coefficients for NO<sub>x</sub> emission factor K<sub>Qnox</sub> and for products of incomplete fuel combustion K<sub>Qco</sub> for average parameters of the engines while in operation are adduced.

Current calculation method, realized in software PolEmiCa, also implemented the recommendations of ICAO Doc9889 [12] for emission factor assessment, including the recommendations for aircraft engine emission.

The efficiency of the temperature (seasonal) factor account for pollution inventory produced by aircraft in airport area is shown in **Table 2** by matching the outcomes of calculation from previous and new calculation techniques [19].

## 2.2 Jet transport model

There are different types of engines installed on civilian aircraft currently: turbojet (TJE), turbofan (TFE), turboprop (TPE), and piston (PE). The process of contaminant transport by engine jet is described by the theory of turbulent jets [20]. The restrictions on the use of this theory are satisfied completely in the current task [21]: efflux from a jet engine is a very complex fast flow of hot gas, it is nonuniform, turbulent, and has various velocity scales and chemical reactions; the gas flow in jet is usually isobaric process, the pressure in the jet flow is equal to the atmospheric pressure, which is corresponding to the nature of incompressible flow; the Mach number of jet flow at outlet nozzle of the engine does not exceed 1; and the Reynolds number for the flow is rather large  $U_0 D_0 / \nu > 10^5$ , and the initial turbulence in the jet flow is quite moderate. For majority of the calculations, the simplifying preconditions were formulated and used: radial velocity profile has a self-preserving pattern; mechanisms of boundary layer formation near ground surface are not taken into account in this calculation; the external borders of a jet represent linear dependencies; the structure of shear layer is similar to free jet [11].

Temperature, °C	-20	-10	0	+10	+20
Factor K <sub>Qnox</sub>	0,74	0,81	0,88	0,96	1,0
Factor K <sub>Qco</sub>	1,3	1,2	1,1	1,04	1,0

**Table 1.**  
 Average values of aircraft engine emission factor recalculation into actual ambient temperature.

Techniques	CO	HC	NO <sub>x</sub>	PM
Previous	307,000.1	104,200.	16,700.0	3400.0
ICAO LTO	282,754.6	97,139.2	18,621.1	2859.4
Actual LTO for considered airport	185,055.1	59,556.4	16,869.1	2207.3
Actual LTO for considered airport + temperature factor	190,246.1	61,254.1	15,984.1	2207.3

**Table 2.**  
 Calculated aircraft engine pollution, kg.



The conditions of jet outflow define the type of its physical model and appropriate algorithm of its parameters calculation. The choice of the model depends on the direction of the jet at exhaust nozzle relative to the direction of the wind and/or airplane motion and from the speeds of the jet, airplane, and wind. The initial parameters for jet calculations are: slipstream flow parameter  $m = U_H/U_0$ , where  $U_0$  is the velocity of the jet at engine nozzle,  $m \cdot s^{-1}$  and  $U_H$  is the speed of an external air flow,  $m \cdot s^{-1}$ ;  $U_H = U_W + U_{PL}$ , where  $U_W$  is the wind speed,  $m \cdot s^{-1}$  and  $U_{PL}$  is the airplane speed,  $m \cdot s^{-1}$ ;  $N_{en}$  – number of the engines in operation, angle between vectors of wind and jet speeds  $\psi$ , grad. For ground stages of LTO cycle in airport area, the slipstream parameter  $m < 1$ ; therefore, in most cases, it is possible to take advantage of semiempirical modeling of the nonisothermal-free jets.

Turbulent-free jet can be divided into three stages: initial (potential core), transitive (flow development region), and developed (fully developed flow) [20]. Their boundaries along the length of jet axis  $S$  and their expansion  $R$  (on considered sites) are defined by the formulas [11, 20, 22]:

- **for an initial stage:**

$$\bar{S}_{IN} = (11.5 - 3.5 \times Q_T) \times (1 + 2.5 \times m); \bar{R}_{IN} = 0.27 \times \bar{S}_{IN} \quad (3)$$

- **for a transitive stage:**

$$\bar{S}_T = 1.5 \times \bar{S}_{IN}; \bar{R}_T = 1.5 \times \bar{R}_{IN} \quad (4)$$

- **for the fully developed stage:**

$$\bar{S}_B = 12.4 \times Q_T^{-1/2} \times (1 - m)/m + \bar{S}_T; \bar{R}_B = 2.728 \times (Q_T m)^{-1/2} + \bar{R}_T \quad (5)$$

where  $\bar{S} = S/R_0$  and  $\bar{R} = R/R_0$ ;  $R_0$  is the radius of engine exhaust nozzle;  $m$  is the slipstream flow parameter; and  $Q_T = T_0/T_A$ , where  $T_0$  and  $T_A$  are the temperature of the jet and atmosphere, K. Parameter  $Q_T$  for modern engines changes within the limits of 1.15–2 for the operational settings of engine power.

The stage of a jet, which is defined by boundary  $S_B$  (6), determines a point  $(X_E, Y_E, Z_E)$  on a jet axis, where centerline flow speed  $U_m$  and the wind speed  $U_W$  become equal. From this point, it is assumed that atmospheric turbulence and wind play a dominant role in the plume behavior and its further dispersion, while the jet parameters influence is not already sufficient at this stage of plume development.

At point  $(X_E, Y_E, Z_E)$ , a jet center-line due to buoyancy effect takes height of plume rise (it is equal to effective height of source  $H$  in (1) and (2)) [11, 20, 22]:

$$Z_E = h_{EN} + \Delta h_A, \quad (6)$$

where  $h_{EN}$  is a height of engine installation (of their axis above a ground surface), m and  $\Delta h_A$  is a height of jet rise, m.

For an estimation of the buoyancy characteristics, the Archimedes number is introduced:

$$Ar_0 = 2 \times g \times R_0 \times (Q_T - 1) / U_0^2, \quad (7)$$

The height of the jet is given by the empirical relationship [23]:

$$\Delta h_A = 0.013 \times Ar_0 \times \bar{X}_A^3 \times R_0, \quad (8)$$

where  $\bar{X}_A = X_A/R_0$ ,  $X_A$  is the longitudinal coordinate of jet axis curved by buoyancy effect,  $m$  (**Figure 1**) and can be calculated by the following formula:

$$\bar{X}_A = \left\{ \left( 1 + 0.156 \times Ar_0 \times \bar{S}_A^2 \right)^{1/2} - 1/0.078 \times Ar_0 \right\}^{1/2}. \quad (9)$$

The concentration is changed along the length of jet in dependence with its type. Taking into account that flow parameter  $m$  in jet is rather small, the concentration  $C$  of the contaminant on a surface  $(X, Z)$  is defined as [20, 22]:

$$C = \frac{2 \times C_0 \times K_C \times K_E}{Q_T^{1/2} \times X} \times \left[ 1 - \left( \frac{Z}{0.23668 \times X} \right)^{1.5} \right]^{1.5}, \quad (10)$$

where  $C_0$  is the concentration at the exhaust nozzle of the engine,  $\mu\text{g}\cdot\text{m}^{-3}$ ;  $K_C = 9.5$  for the free jet,  $K_C = 6.5$ —for an opposite jet; and  $K_E$  takes into account influence of a reflecting surface on straightline characteristics of a jet:  $\hat{h}_{EN} < 20$   $K_E = 1 - 0.025\hat{h}_{EN}$ , at  $\hat{h}_{EN} \geq 20$ ,  $K_E = 1$ , where  $\hat{h} = h/R_0$ .

Considered version of complex model PolEmiCa is based on a semiempirical model of turbulent jets and not taking into account ground surface impact on jet structure and its behavior [11]. It was argued that development of three-dimensional model of exhaust gases jet from aircraft engine near the ground is an important research topic for airport LAQ [24–26].

A three-dimensional model of a jet was generated in Fluent 6.3 by using large Eddy simulation (LES) method to reveal the unsteady ground vortices and turbulence characteristics of fluid flow, to investigate transient parameters of hot gases in jet and their dispersion.

The jet from aircraft engine exhaust near ground surface is corresponding to a wall jet if an aircraft is moving on this surface. Numerical simulation of wall jets was performed in Fluent 6.3 for engine NK-8-2 U of the aircraft Tupolev-154 for different operational conditions.

For the considered task, a computational domain was built to simplify the problem and optimize the mesh distribution where it is needed mostly (i.e., near the engine exhaust and ground surface) (**Figure 8**).

The zone of ground vortices formation—between ground surface and aircraft engine exhaust nozzle—is characterized by structured mesh with higher resolution, with an aim to investigate the ground vortices generation processes and basic mechanisms of boundary layer formation, ground surface impact on fluid flow mechanics, and particularly Coanda effect occurrence. Zone of engine nozzle exhaust is discretized using a very fine structured mesh to capture the jet development pattern and its vortices structure [24, 25].

For considered task, the boundary conditions were specified to the boundaries of the computational domain of jet flow field (**Figure 9**).

LES provides an approach inside which large eddies are explicitly resolved in time-dependent simulation using low-pass-filtered Navier-Stokes equations [25]. Smagorinsky's subgrid model was set to model the smaller eddies (fluctuation component of instantaneous velocity of modeling fluid flow) that are not resolved in the LES. All the calculations were made with a second-order discretization.

Comparison of results from numerical simulations of free and wall jets for engine idle operation ( $U_0 = 50 \text{ m}\cdot\text{s}^{-1}$ ;  $T_0 = 343 \text{ K}$ ) revealed some differences in their structures and properties.

Axial velocity profiles based on Fluent 6.3 results show (**Figure 10**) a substantial difference between the wall and free jet. First, the decay rate is 40–50% higher for

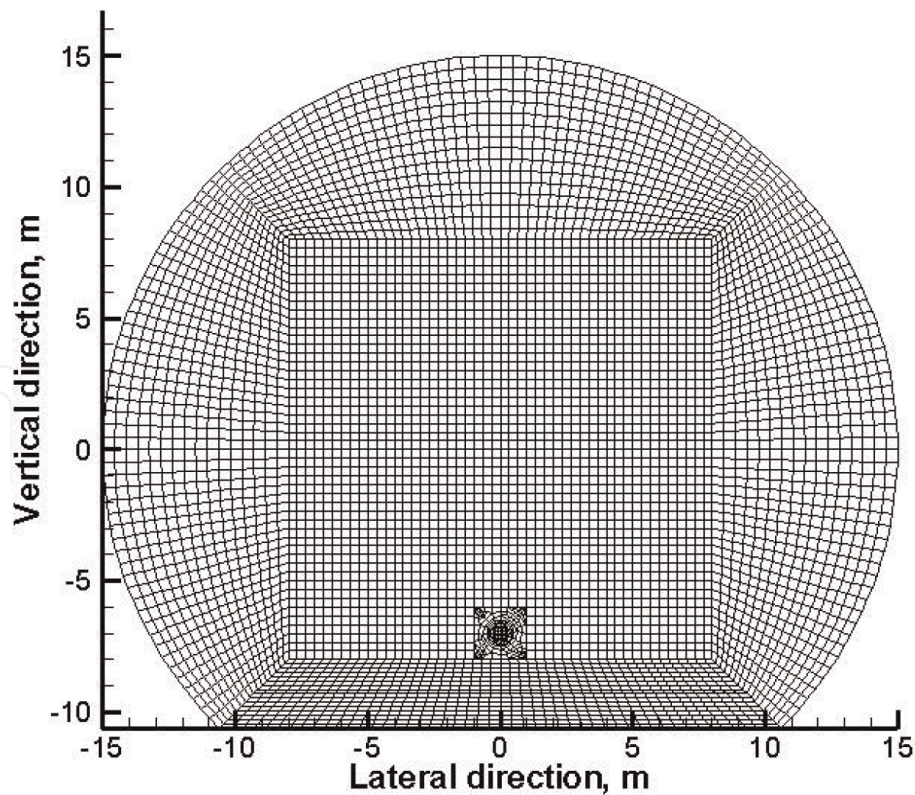


Figure 8.  
Geometry model and computational mesh visualization in vertical plane.

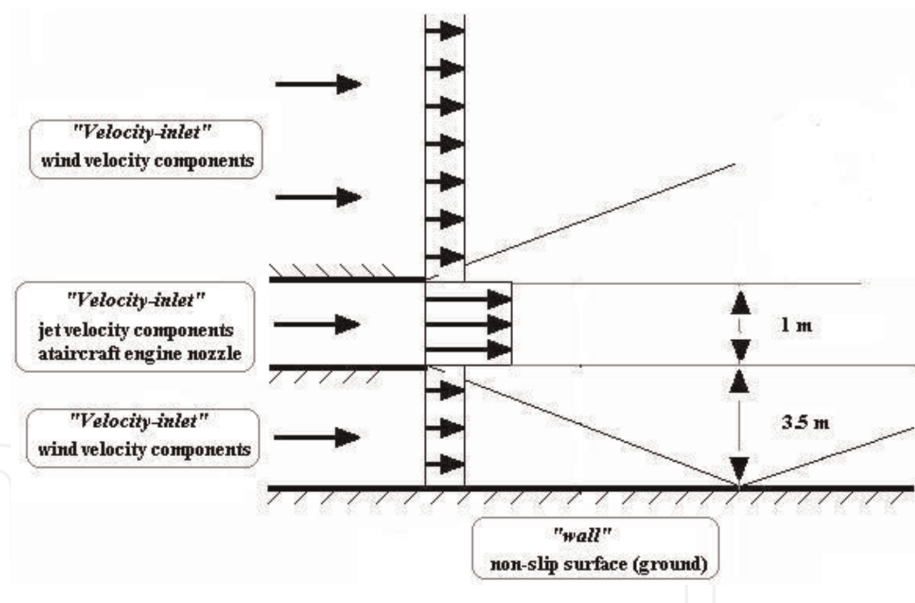
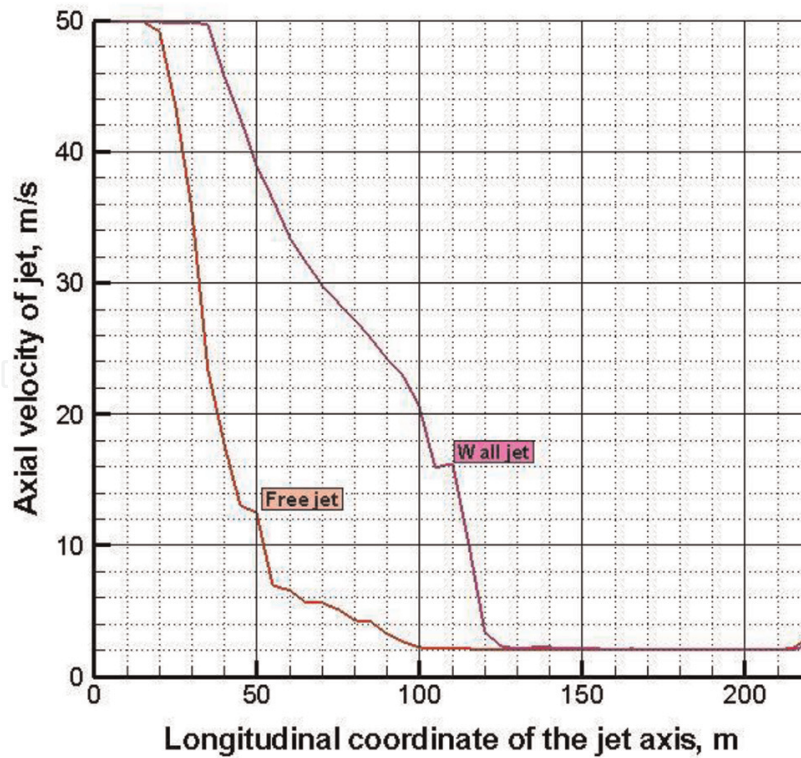


Figure 9.  
Boundary conditions for CFD simulations of exhaust gases of jet from aircraft engine near ground.

free jet than for the wall jet. In the case of wall jet, the maximum velocity is high and equal to 50% of initial velocity at a distance of 90 diameters of the jet penetration, whereas the free jet is relatively slow and equal only to 10% of the velocity at exhaust nozzle of the engine, **Figure 10**. Second, the wall jet penetrates deeper ( $S_{Bwall} \approx 150$  m) than the free jet ( $S_{Bfree} \approx 100$  m) (**Figure 11**). As shown in **Figure 12**, jet arises over the ground surface due to buoyancy effect much faster (longitudinal coordinate,  $X_A = 65$  m) and higher for free jet (height of plume rise,  $\Delta h_A = 17.8$  m), than in case of wall jet ( $X_A = 135$  m,  $\Delta h_A = 14$  m).

The same differences in the structure and properties of free and wall jets were revealed for different operational conditions ( $U_0 = 100 \text{ m}\cdot\text{s}^{-1}$ ;  $T_0 = 343 \div 673 \text{ K}$ ).





**Figure 10.**  
 Maximum velocity decay along the axis of the free and wall jets.

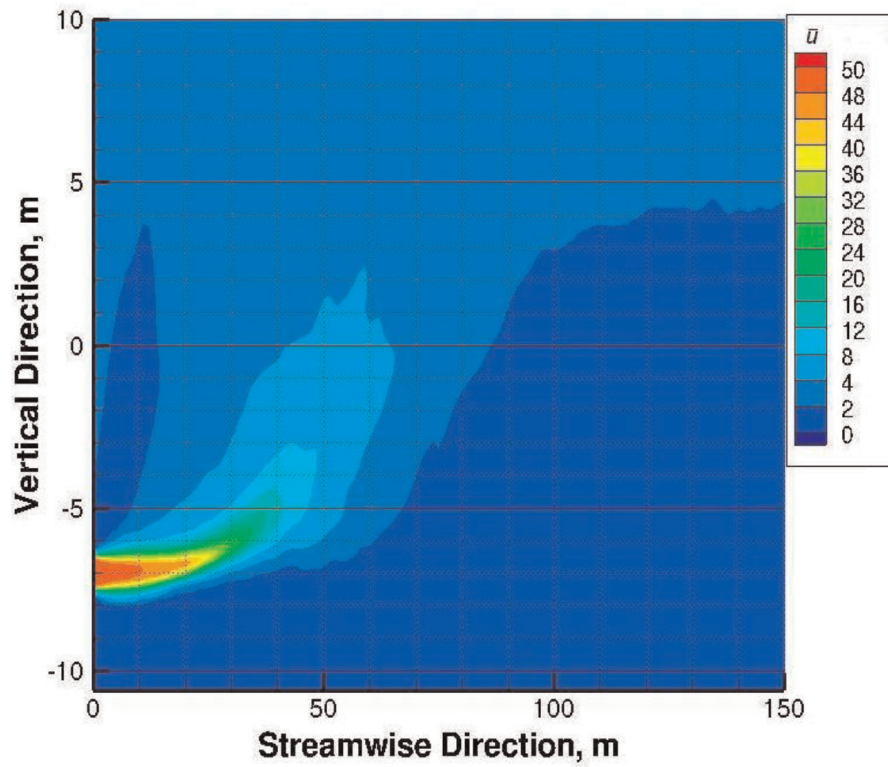
The ground surface sufficiently impacts on jet's structure and behavior. Numerical simulations of wall jet by Fluent 6.3 defined a decrease of buoyancy effect of height rise, which is 3–5 times less (**Figure 13a**) and an increase of longitudinal coordinate of jet penetration by 30%, (**Figure 13b**).

Comparison of the calculated parameters of the jet (height and longitudinal coordinate of jet axis arise due to buoyancy effect, length of the jet penetration) by Fluent 6.3 and semiempirical model for aircraft engine jets implemented in complex model PolEmiCa proves the found trend of the jet behavior. Thus, the including the ground impact on the jet structure and its behavior by Fluent 6.3, provides longitudinal coordinate increase and height reduction of buoyancy effect.

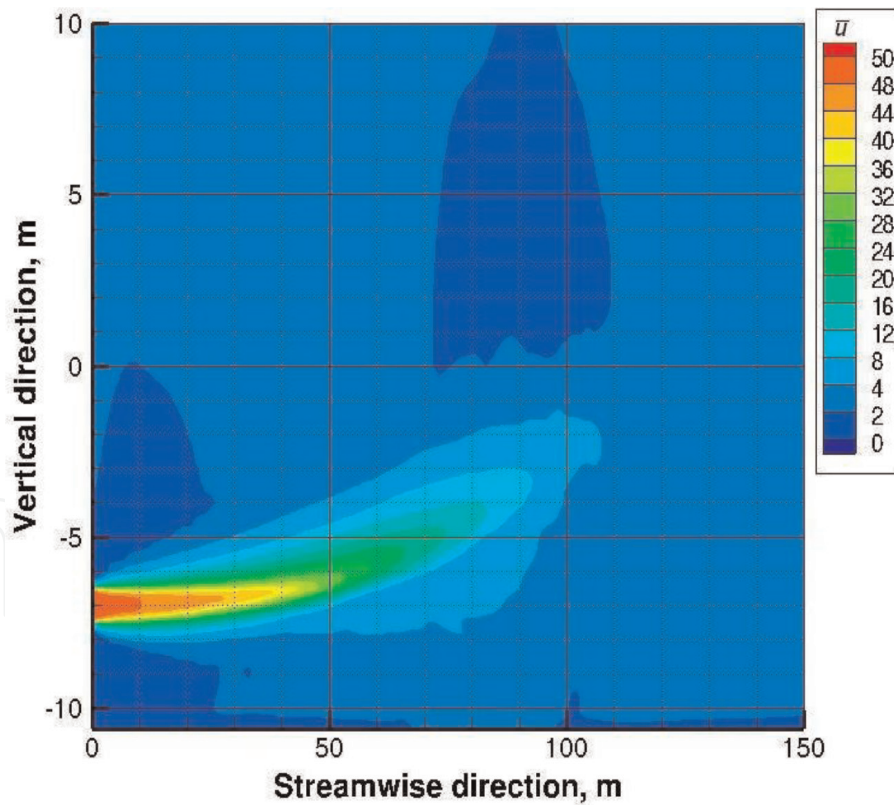
### 2.3 Dispersion model

The basic model equation for definition of instantaneous concentration  $C$  at any moment  $t$  in point  $(x, y, z)$  from a moving source from a single exhaust event with preliminary transport by jet on distance  $X_A$  and rise on total altitude  $H$  (**Figure 4**) and dilution of contaminants by jet ( $\sigma_0$ ) has a form [11, 19]:

$$C(x, y, z, t) = \frac{Q \exp \left[ -\frac{(x-x')^2}{2\sigma_{x0}^2 + 4K_x t} - \frac{(y-y')^2}{2\sigma_{y0}^2 + 4K_y t} \right]}{\left\{ 8 \pi^3 [\sigma_{x0}^2 + 2K_x t] [\sigma_{y0}^2 + 2K_y t] \right\}^{1/2}} \times \left\{ \frac{\exp \left[ -\frac{(z-z'-H)^2}{2\sigma_{z0}^2 + 4K_z t} \right] + \exp \left[ -\frac{(z+z'+H)^2}{2\sigma_{z0}^2 + 4K_z t} \right]}{[\sigma_{z0}^2 + 2K_z t]^{1/2}} \right\} \quad (11)$$



(a)



(b)

**Figure 11.** Mean velocity contours for (a) free jet and (b) wall jet in streamwise direction after 10 s.

where  $K_X$ ,  $K_Y$ ,  $K_Z$  are the diffusion factors ( $\text{m}^2 \cdot \text{s}^{-1}$ ) for atmosphere turbulence along three axes, axis  $OX$  is directed along wind direction. Aircraft is considered as a moving emission source, thus current coordinates  $(x', y', z')$  of the emission source in movement during time  $t'$  are defined as:



$$\begin{aligned} x' &= x_0 + u_{PL}t' + 0.5a_{PL}t'^2 + u_w(t + t'); \\ y' &= y_0 + v_{PL}t' + 0.5b_{PL}t'^2; \\ z' &= z_0 + w_{PL}t' + 0.5c_{PL}t'^2. \end{aligned} \quad (12)$$

where  $x_0, y_0, z_0$  are initial coordinates of the source, m;  $u_{PL}, v_{PL}, w_{PL}$  are vector components of source speed,  $\text{m}\cdot\text{s}^{-1}$ ;  $a_{PL}, b_{PL}, c_{PL}$  are vector components of source acceleration,  $\text{m}\cdot\text{s}^{-2}$ ; and  $u_w$  is the wind speed,  $\text{m}\cdot\text{s}^{-1}$ .

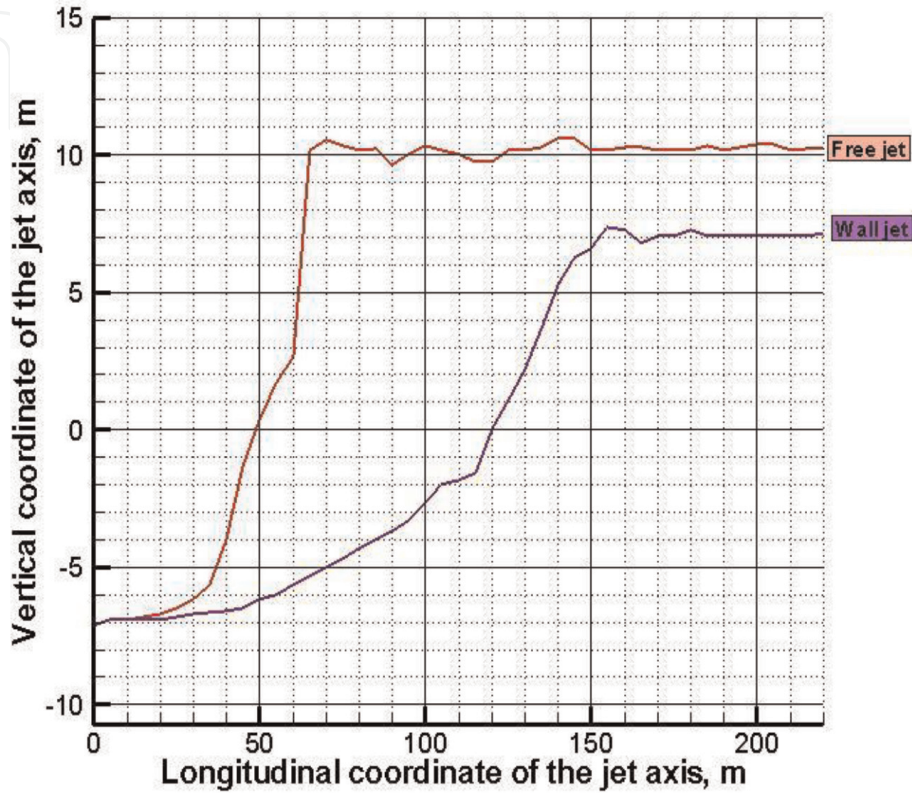


**Figure 12.**  
 Buoyancy effect of free and wall jets: longitudinal and vertical coordinates of jet axis.

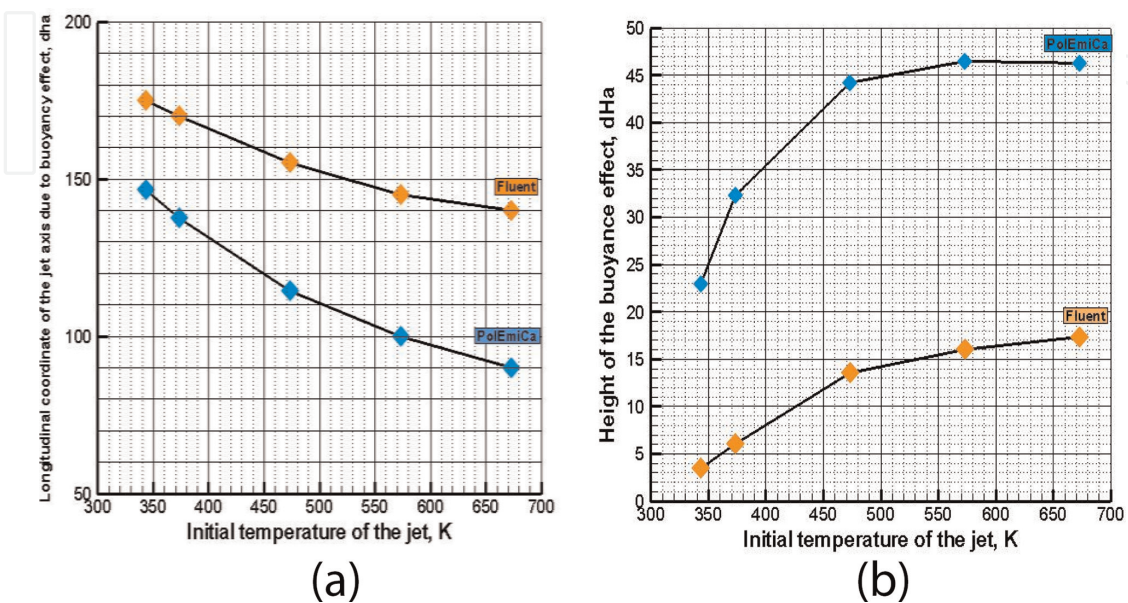


**Figure 13.**  
 Comparison of buoyancy effect parameters calculated by Fluent 6.3 and complex model PolEmiCa: longitudinal coordinate (a) and height of jet rise (b).

According to considered formula (11), a dispersion model integrates engine emission model and jet transport model via including the following parameters:

$Q$ —emission rate is provided by engine emission model and includes influence operational and meteorological conditions [17–19].

$H$ —height of buoyancy effect and horizontal  $\sigma_x^2$ ,  $\sigma_y^2$  and vertical  $\sigma_z^2$  dispersion are provided by *jet transport model* [24–26].

In other words, engine emission model and jet transport model provide input data to calculate concentration values by the dispersion model.

The development of three-dimensional model of wall jet by using CFD tool (Fluent 6.3) allows to include the ground impact on basic parameters of the exhaust gases jet (i.e., plume buoyancy effect, length, and dispersion characteristics) for further dispersion modeling (11). It may be concluded that using the CFD tool allows us to improve the PolEmiCa model by taking into account the impact of ground surface on the jet structure and its behavior. So, it means that the improvement is achieved with input parameters for further dispersion calculation.

### 3. Measurement of air pollution produced by aircraft engine emissions

The verification of the PolEmiCa model with measurement data was done initiatively for trials made in airports of Athens (Greece, 2007) [27] and Boryspil (Ukraine, 2012) [28]. In both cases, the comparisons were quite good, showing appropriate correspondence of the model to subject of assessment.

Comparison between calculated and measured NOx concentrations (averaged for 1 min) in aircraft engine plume under real operation conditions (aircraft accelerating on the runway during takeoff stage of flight) at Athens airport is shown in **Table 3** and **Figure 14**.

Besides, results were defined for the cases with and without jets from the engines to show that with jets, they are more equal (by 17%) to measured data,

№	Aircraft	Engine	Calculated concentration		Measured concentration	
			NOx (delta), $\mu\text{g}/\text{m}^3$		NOx (delta), $\mu\text{g}/\text{m}^3$	
			With jet	Without jet	Value	Error
1	B737-3YO	CFM56-3C1	27,43	30,01	31,8	3,2
2	B737-3Q8	CFM56-3B2	30,7	33,50	28,0	2,8
3	B737-45S	CFM56-3B2	29,76	27,95	23,6	2,4
4	B737-4Q8	CFM56-3B2	31,28	34,93	56,9	5,7
5	A-310	CF6-80C2A8	88,86	122,12	86,1	8,6
6	A-319	CFM56-5B5	29,85	32,27	26,9	2,7
7	B747-230	CF6-50E2	163,63	205,37	82,5	8,2
8	A-321-211	CFM56-5B-3	81,78	89,74	43,3	4,3
9	A320-214	CFM56-5B-4	49,99	52,29	16,4	1,6
10	B737-33A	CFM56-3B1	25,5	27,95	11,5	1,1

**Table 3.**

*Measurement results by TE42C-TL96 system and calculation results by PolEmiCa model of NOx concentration in plume from aircraft engine emission for maximum operation mode.*

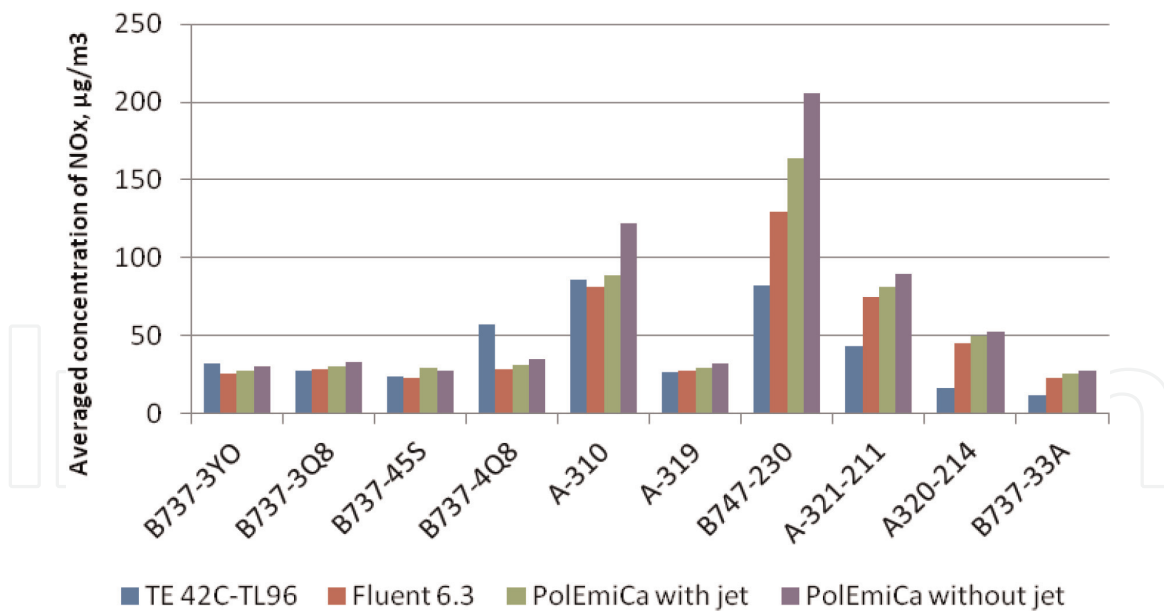


**Figure 14.** Comparison of measured and modeled averaged concentrations of NOx (for a period of 1 min) under takeoff conditions (maximum operation mode of aircraft engine).

because impact of jet basic parameters (buoyancy effect and dispersion characteristics) on concentration distribution was estimated by complex model PolEmiCa (Table 3 and Figure 14). Comparison between measurements and the PolEmiCa/Fluent 6.3 model is significantly better (by 20%), because lateral wind and ground impact on jet parameters (height of buoyancy effect, jet length penetration, and plume dispersions) were included in the model.

The better agreement was obtained between the calculated and measured instantaneous concentration (averaged for 3 s) in aircraft engine jet under real operation conditions (aircraft accelerating on the runway and takeoff) at Boryspil airport.

As shown from Table 4 and Figure 15, the modeling results for each engine are in good agreement with the results of measurements by the AC3 2 M system due to taking into account the jet- and plume regime during experimental investigation at Boryspil airport. Also, using CFD code (Fluent 6.3) allows to improve results by 30% (coefficient of correlation,  $r = 0.76$ ) by taking into account lateral wind and ground impact on jet parameters.

Aircraft	Aircraft engine	ELAN		AC3 2 M		PolEmiCa CFD (Fluent 6.3)		PolEmiCa		
		Peak 1	Peak 1	Background	3 M	6 M	1 engine	All engines	1 engine	All engines
		NOx	NOx	NOx	NOx	NOx	NOx	NOx	NOx	NOx
BAE147	LY LF507-1H	38	35	1,70	22,067	33,9	35,1	70,46	48,9	202,3
A321	CFM56-5B3/P	39	39	0,72	44,00	54,2	90,85	182,90	184,2	371,2
B735	CFM-563C1	40	45	0,77	94,095	76,57	60,03	120,91	35,3	71,10
B735	CFM56-3B1	45	41	1,74	29,20	23,4	42,34	85,30	33,7	67,76

**Table 4.** Comparison measured (AC3 2 M, ELAN) and calculated concentration (averaged for 3 s) of NOx produced by aircraft engine emissions at accelerating stage on the runway.

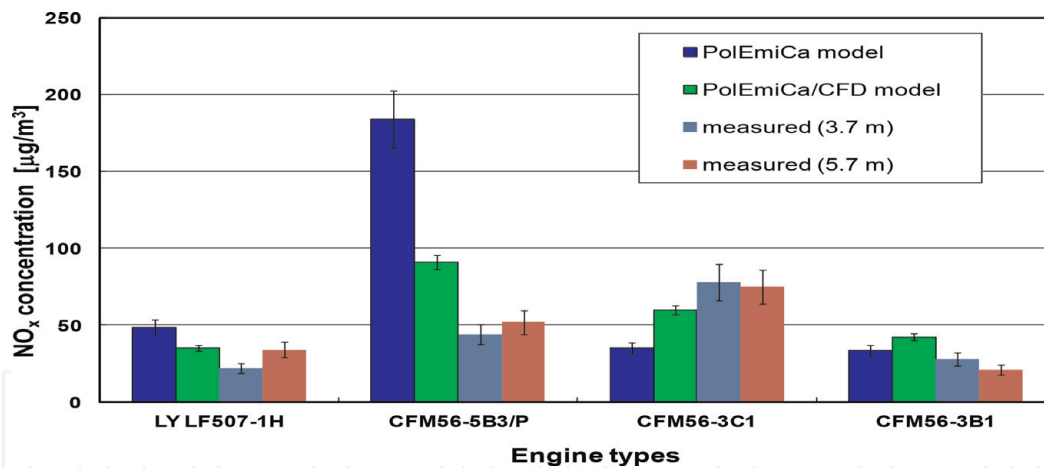


**Figure 15.** Comparison of the PolEmiCa and PolEmiCa/CFD model results with the measured NO<sub>x</sub> concentration at different heights for selected aircraft engines under maximum operation mode.

## 4. Conclusions

Analysis of inventory emission results at the major European and Ukrainian airports highlighted that aircrafts (during approach, landing, taxi, takeoff and initial climb of the aircraft, engine run-ups, etc.) are the dominant source of air pollution in most cases under consideration. The aircraft is a special source of air pollution. Thus, the method for LAQ assessment of the airports has to take in mind few features of the aircraft during their landing-takeoff cycle (LTO), which defines emission and dispersion parameters of the considered source.

CFD numerical simulations of aircraft engine exhaust jet near to ground surface show that structures, properties, and fluid mechanics of jets are influenced by the ground surfaces, providing longer penetration, less rise, and appropriate dispersion parameters of the jets, and accordingly little bit higher concentrations of air pollution. So, using results obtained from CFD simulations (Fluent 6.3) of aircraft engine jet dynamics allow us to improve LAQ modeling systems (improved version of PolEmiCa).


Comparison of measured and modeled NO<sub>x</sub> concentrations in the plumes from aircraft engines was significantly improved (by 20%—at Athens and by 30%—at Boryspil airports) by taking into account lateral wind and ground impact on jet parameters (height of buoyancy effect, jet length penetration, and plume dispersions).

### Author details

Oleksandr Zaporozhets and Kateryna Synylo\*  
National Aviation University, Kyiv, Ukraine

\*Address all correspondence to: [synyka@gmail.com](mailto:synyka@gmail.com)

### IntechOpen

© 2019 The Author(s). Licensee IntechOpen. This chapter is distributed under the terms of the Creative Commons Attribution License (<http://creativecommons.org/licenses/by/3.0>), which permits unrestricted use, distribution, and reproduction in any medium, provided the original work is properly cited. 



## References

- [1] EEA. 2016. European Aviation Environmental Report. Available from: <https://ec.europa.eu/transport/sites/transport/files/european-aviation-environmental-report-2016-72dpi.pdf> [Accessed: 29 January, 2016]. ISBN: 978-92-9210-197-8
- [2] Carslaw D, Beevers S, Ropkins K, Bell M. Detecting and quantifying aircraft and other on-airport contributions to ambient nitrogen oxides in the vicinity of a large international airport. *Atmospheric Environment*. 2006; **40**(28):5424-5434
- [3] Peace H, Maughan J, Owen B, Raper D. Identifying the contribution of different airport related sources to local urban air quality. *Environmental Modelling and Software*. 2006; **21**(4): 532-538
- [4] Jung K, Artigas F, Shin J. Personal, indoor, and outdoor exposure to VOCs in the immediate vicinity of a local airport. *Environmental Monitoring and Assessment*. 2011; **173**(1):555-567
- [5] Nicholas Rand. Heathrow Air Quality Strategy, 2011–2020. Available from: [https://www.heathrow.com/file\\_source/Company/Static/PDF/Communityandenvironment/air-quality-strategy\\_LHR.pdf](https://www.heathrow.com/file_source/Company/Static/PDF/Communityandenvironment/air-quality-strategy_LHR.pdf)
- [6] Celikel A, Duchene N, Fleuti E, Fuller I, Hofman P, Moore T, and Silue M. Airport local air quality studies: Zurich Airport Emissions Inventory Using Three Methodologies. 2004. Available from: [https://www.eurocontrol.int/eec/public/standard\\_page/DOC\\_Conf\\_2005\\_007.html](https://www.eurocontrol.int/eec/public/standard_page/DOC_Conf_2005_007.html) [cited: July 2005]
- [7] Schäfer K, Jahn C, Sturm P, Lecher B, Bacher M. Aircraft emission measurements by remote sensing methodologies at airports. *Atmospheric Environment*. Elsevier; 2003; **37**:5261-5271
- [8] Herndon S, Jayne J, Lobo P. Commercial aircraft engine emissions characterization of in-use aircraft at Hartsfield Jackson Atlanta international airport. *Environmental Science & Technology*. 2008; **42**(6): 1877-1883
- [9] Fraport Environmental Statement (2014). Including the Environmental Program, until 2017. Fraport AG; 2015. pp. 24-30
- [10] Umweltbericht. Umwelterklärung 2008 mit Umweltprogramm bis 2011 für den Standort Flughafen Frankfurt Main. Fraport AG; 2008. pp. 100-104
- [11] Zaporozhets O, Synylo K. PolEmiCa —tool for air pollution and aircraft engine emission assessment in airport. In: *The Proceedings of the Second World Congress “Aviation in the XXI-st Century”*; Ukraine: Kyiv; 2005. pp. 4.22-4.29
- [12] ICAO Doc9889. AirportAirQuality. 1st ed. INTERNATIONAL CIVIL AVIATION ORGANIZATION 999 University Street, Montréal, Quebec, Canada; 2011. 200 p
- [13] Emissions and Dispersion Modelling System (EDMS). Reference Manual. FAA-AEE-01-01. U.S. Department of Transportation Federal Aviation Administration. Washington, D.C.: CSSI, Inc; 2002
- [14] Janicke Consulting. LASPORT version 1.3 Reference Book; 2005. 93 p
- [15] Zaporozhets O. 2015. PolEmiCa Local Air Quality Model Evaluation/O. In: Zaporozhets K. Synylo. ABIA2015: XII міжнародна наук.-техн. конф., 2015: збірник матеріалів—К., – С.29.12–29.15. (19)
- [16] ICAO data Bank of Aircraft Engine Emissions. Montreal: ICAO. Doc. 9646-AN/943; 1995. 152 p



- [17] Zaporozhets O, Synylo K. Improvements on aircraft engine emission and emission inventory assessment inside the airport area. *Energy Journal (SCOPUS)*. 2017;5: 1350-1357
- [18] Zaporozhets O, Synylo K. Operational conditions influence on aircraft engine emission and pollution inside the airport. *International Journal of Sustainable Aviation*. 2017;3(1):1-17
- [19] Synylo K, Zaporozhets O. PolEmiCa model for local air quality assessment in airports. *Community Modeling and Analysis System, 16th Annual CMAS Conference*; 23–25 October, 2017. Chapel Hill, NC, USA: University of Northern Carolina. 6 p
- [20] Abramovich GI. *The Theory of Turbulent Jets*. Moscow: Physmatgiz; 1960. 716 p
- [21] Tokarev VI, Zaporozhets OI. Mathematical principles of modeling of atmospheric contamination processes by effluents of harmful substances at maintenance of aircrafts. In: *State and Perspective of Activities on Environment Protection in Civil Aviation*. Moscow: GosNIIGA; 1987. pp. 53-60
- [22] Zaporozhets O. Evaluation of preliminary dispersion of effluents of contaminant substances by jets. In: *Problems of Environment Protection at Intensification of Aircraft Productions*. Kyiv: KIECA; 1986. pp. 42-51
- [23] Taliev VN. *Aerodynamics Ventilation—M*; 1979. 295 p
- [24] Pope Turbulent Flows. Cornell University, New York: Cambridge University Press; 2000. 841 p
- [25] Zaporozhets O, Synylo K, Fröhlich J, Stiller J. Improvement of airport local air quality modeling. *Journal of Aircraft*. 2017;54(5):1750-1759
- [26] Zaporozhets O, Synylo K. New and improved LAQ models for assessment of aircraft engine emissions and air pollution in and around airports. On board a sustainable future: ICAO Environmental Report 2016, International Civil Aviation Organization 999 University Montreal, QC, Canada H3C 5H7. 2016. 250p. pp. 82-84
- [27] Zaporozhets O, Wiesen P, Kurtenbach R, Synylo K. Comparison between modelled and measured NO<sub>x</sub> concentrations in aircraft plumes at Athens international airport. *International Journal of Sustainable Aviation*. 2017;4(3):1-17
- [28] Zaporozhets O, Wiesen P, Kurtenbach R, Synylo K. Measurement of aircraft engine emissions inside the airport. In: *The 4th International Conference on Transport, Atmosphere and Climate*; June 2015. Bad Kohlgrub (Germany): Proceedings; 2015. pp. 28-33